

# One-dimensional localization with correlated disorder

C. M. Soukoulis

*Ames Laboratory and Department of Physics and Astronomy, Iowa State University, Ames, Iowa 50011*

M. J. Velgakis

*School of Engineering, Science Department, University of Patras, 26110 Patras, Greece*

E. N. Economou

*Research Center of Crete, P.O. Box 1527, 71110 Heraklion, Crete, Greece*

*& Department of Physics, University of Crete, 71110 Heraklion, Crete, Greece*

(Received 25 March 1994)

A one-dimensional tight-binding model with correlated disorder is studied. The energy dependence of the localization length and the density of states at different correlation lengths and strengths of the disorder are determined. The results show that the localization length increases with increasing correlation lengths, but in addition, a nonmonotonic energy dependence is found. The energy level statistics is also studied.

## I. INTRODUCTION

Most of the theoretical work on Anderson localization has been based on simple tight-binding models, where the diagonal matrix elements  $\epsilon_n$  of the Hamiltonian are independent random variables.<sup>1</sup> The question of statistically correlated matrix elements has not been extensively studied, except in the case of binary-alloy disorder<sup>2-6</sup> in one dimension. Here, it was clearly shown<sup>5,6</sup> that special types of correlated disorder can produce extended states. The results of Ref. 4 have shown that increasing the correlation length may decrease or increase the localization, depending on the type of correlation, the energy, the disorder, the concentration, and the size of the correlation length. The motivation of the studies of correlated disorder is twofold. First, we seek to determine how sensitive, if at all, the results of the localization theory on the correlation are, which are based on the independent random variables. Second, long correlation lengths allow us to map the problem to that of wave propagation in the continuum. The latter is directly related to the interesting question of light localization.<sup>7,8</sup> We would like to determine under which circumstances and to what extent the potential correlation length  $L$  can simply replace the lattice spacing  $a$  in our uncorrelated results.

In this paper, we will generalize the Anderson model of localization to include correlations. The lattice size energies are no longer independent random variables, but they become correlated random variables with a finite-range correlation. The exact model is described in Sec. II. We consider the localization length of this correlated disorder model, the density of states (DOS), and the energy level statistics. For our model, the localization length  $\lambda$  increases with increasing correlation length. In addition, the energy dependence of  $\lambda$  is not monotonic, and maxima appear at nonzero energy values. This behavior can be explained qualitatively by second-order perturbation

theory and by the transmission coefficient studies of an isolated scatterer of size equal to the correlation length  $L$ .

In Sec. II we present our model, a single-orbital-per-site, tight-binding, one-dimensional (1D) model with a correlated diagonal randomness of correlation length  $L$  and with no off-diagonal disorder. In Sec. III we present results of the localization length, the DOS, and the energy level statistics. Finally, in Sec. IV we present a brief summary of our results and our main conclusions.

## II. THE MODEL AND METHOD OF CALCULATIONS

Our tight-binding, one-electron Hamiltonian is given by

$$H = \sum_n \epsilon_n |n\rangle \langle n| + \sum_{n,m} V_{n,m} |n\rangle \langle m|, \quad (1)$$

where  $|n\rangle, |m\rangle$  are atomiclike orbitals centered at the  $n$  and  $m$  sites, respectively, of an infinite one-dimensional lattice of spacing  $a$ . The off-diagonal matrix elements  $V_{n,m}$  vanish unless  $n$  and  $m$  are nearest neighbors and are constant (taken as our unit of energy) otherwise. Thus, the second sum in Eq. (1) is over the nearest neighbors only. The quantities  $\{\epsilon_n\}$  are correlated random variables with zero mean and nonzero correlation  $\langle \epsilon_n \epsilon_m \rangle$ . We consider the following model for the correlation:  $\langle \epsilon_n \epsilon_m \rangle = w^2$  for  $n = m$ , or  $|n - m| \leq L$ , and  $\langle \epsilon_n \epsilon_m \rangle = 0$ , otherwise. Therefore, we have the same value for  $\epsilon_n$  for  $L$  consecutive sites. The different clusters of  $\epsilon_n$  values are given by a rectangular probability of width  $W$ . A typical configuration of the correlated random site energies  $\epsilon_n$  with  $L = 5$  is given in Fig. 1. Notice that for  $L$  consecutive sites,  $\epsilon_n$  is the same and

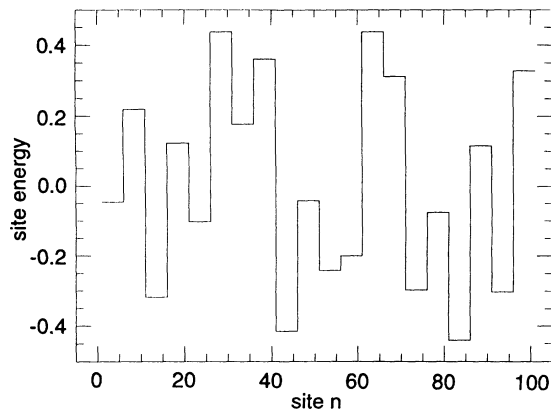


FIG. 1. The behavior of the correlated random site energies  $\epsilon_n$  versus the site  $n$ . The correlation length is  $L = 5$ , and disorder  $W=1$ .

given by a rectangular probability of width  $W$ . If the correlation length is equal to one, then one recovers the uncorrelated case. Our main concern in this study is to investigate how the localization length, the DOS, and the energy level statistics behave as functions of the correlation length  $L$ .

The localization length  $\lambda$  is calculated numerically,

by iterating Eq. (2). To evaluate  $\lambda$ , we have generated numerically  $M$  sets of random variables  $\{\epsilon_n\}$ , ( $n = 1, 2, \dots, N$ ) according to the probability distribution for  $\epsilon_n$ . For each set, we calculated numerically the transmission amplitude  $\bar{t}_N$  (the transmission coefficient is  $|\bar{t}_N|^2$ ). The localization length is given by

$$\frac{1}{\lambda} = -\frac{1}{N} \langle \ln |\bar{t}_N| \rangle, \quad (2)$$

where the average was performed over the  $M$  members of the ensemble. The result is independent of  $N$  as long as  $N$  is greater than the correlation length  $L$ . However,<sup>1</sup> the standard deviation of  $\ln |\bar{t}_N|$  over its average value behaves like  $(\lambda/N)^{1/2}$  for  $N \gg \lambda$  and is constant for  $N \ll \lambda$ . Thus, from the numerical point of view, more accurate results are obtained if  $N \gg \lambda$ .  $M$  was usually chosen equal to 5000, but higher values were also used. The size  $N$  of the system was taken to be equal to 50 000.

The DOS can be obtained either by direct diagonalization of the Hamiltonian  $H$  or by calculating the diagonal matrix element  $G$  of the Green's function, where  $G = \langle m | (E + is - H)^{-1} | m \rangle$  as  $s \rightarrow 0^+$ . To evaluate  $G$  numerically, one can employ the so-called renormalized perturbation expansion which is reduced in one dimension to an iterative procedure.<sup>1</sup> Once  $G$  is calculated, one obtains the DOS  $n(E)$  as  $n(E) = -\text{Im}(G)/\pi$ . Both

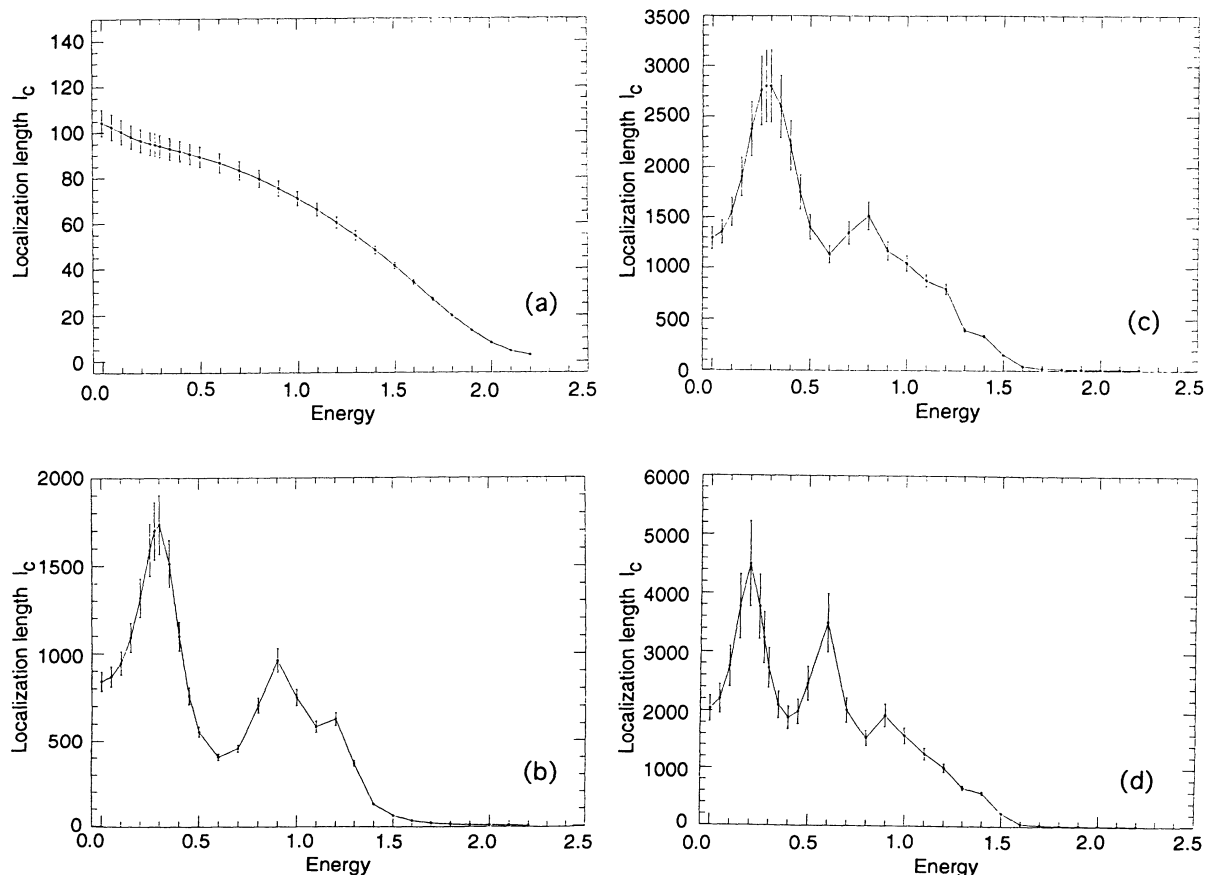


FIG. 2. The localization length  $\lambda$  versus energy for a random system of size  $N = 10000$ , disorder  $W = 1$ , and correlation length  $L = 1$  (a),  $L = 5$  (b),  $L = 10$  (c), and  $L = 15$  (d). The number of random configurations is  $M = 5000$ .

methods give similar results. In each of the methods, one needs to computer generate  $M$  different sets of random variables  $\{\epsilon_n\}$ , ( $n = 1, 2, \dots, N$ ), taken from the ensemble defined by the probability distribution of  $\{\epsilon_n\}$ .  $M$  was usually chosen equal to 200, but higher values were also used. The average DOS was then calculated by averaging over the  $M$  numbers of the ensemble.

Finally, in order to investigate the energy level spacing distribution  $P(S)$ , we numerically diagonalized the Hamiltonian (1) for a given system length  $N$ , correlation length  $L$ , and disorder  $W$ . After the exact diagonalization, the distribution of the energy level spacing  $P(S)$  was plotted. In this case, too, we had to computer generate  $M$  different sets of the random variables  $\{\epsilon_n\}$ ,  $n = 1, 2, \dots, N$ . Therefore,  $M$  different systems were diagonalized for each combination of the parameters  $N$ ,  $L$ , and  $W$ . Then the average  $P(S)$  was obtained by averaging over the  $M$  members of the ensemble. For the uncorrelated case, in agreement with previous calculations,<sup>9-13</sup> we observed for a small disorder (i.e., when the localization length  $\lambda$  is larger than the size of the system  $N$ ) the effect of the level repulsion, where  $P(S)$  is extremely close to the Wigner probability distribution. With increasing disorder (i.e., when  $\lambda \ll N$ ),  $P(S)$  follows the Poisson probability distribution. The role of the correlation in our model is to effectively in-

crease the localization length and therefore, to observe only a Wigner-like probability distribution for  $P(S)$ .

### III. RESULTS AND DISCUSSION

In Fig. 2 we plotted the localization length  $\lambda$  versus the energy  $E$  for different values of the correlation length  $L$ , for the size of the system  $N=10\,000$  and with the strength of the disorder  $W = 1$ , where  $W$  is the width of the rectangular probability distribution of the correlated random variables  $\{\epsilon_n\}$ . The standard deviation  $w^2$ , which is equal to  $\langle \epsilon_n \epsilon_m \rangle$  for  $|n - m| \leq L$ , is related to  $W$  by the following relation:  $w^2 = W^2/12$ . The number  $M$  of different random configurations  $\{\epsilon_n\}$  is equal to 5000, to ensure good statistics. In Fig. 2(a),  $\lambda$  versus  $E$  for the uncorrelated case is shown. Notice that  $\lambda$  has a maximum at the center of the band ( $E = 0$ ) and drops monotonically to lower values as the energy  $E$  approaches the end of the band ( $E = 2$ ). This behavior has been extensively studied and is well known.<sup>1</sup> Notice that with the introduction of the correlation,  $\lambda$  dramatically increases for all values of  $E$ . In addition, a new, but very interesting, structure appears in the energy dependence of  $\lambda$  for all values of  $L$ .  $L = 5$  in Fig. 2(b),  $L = 10$  in Fig. 2(c), and

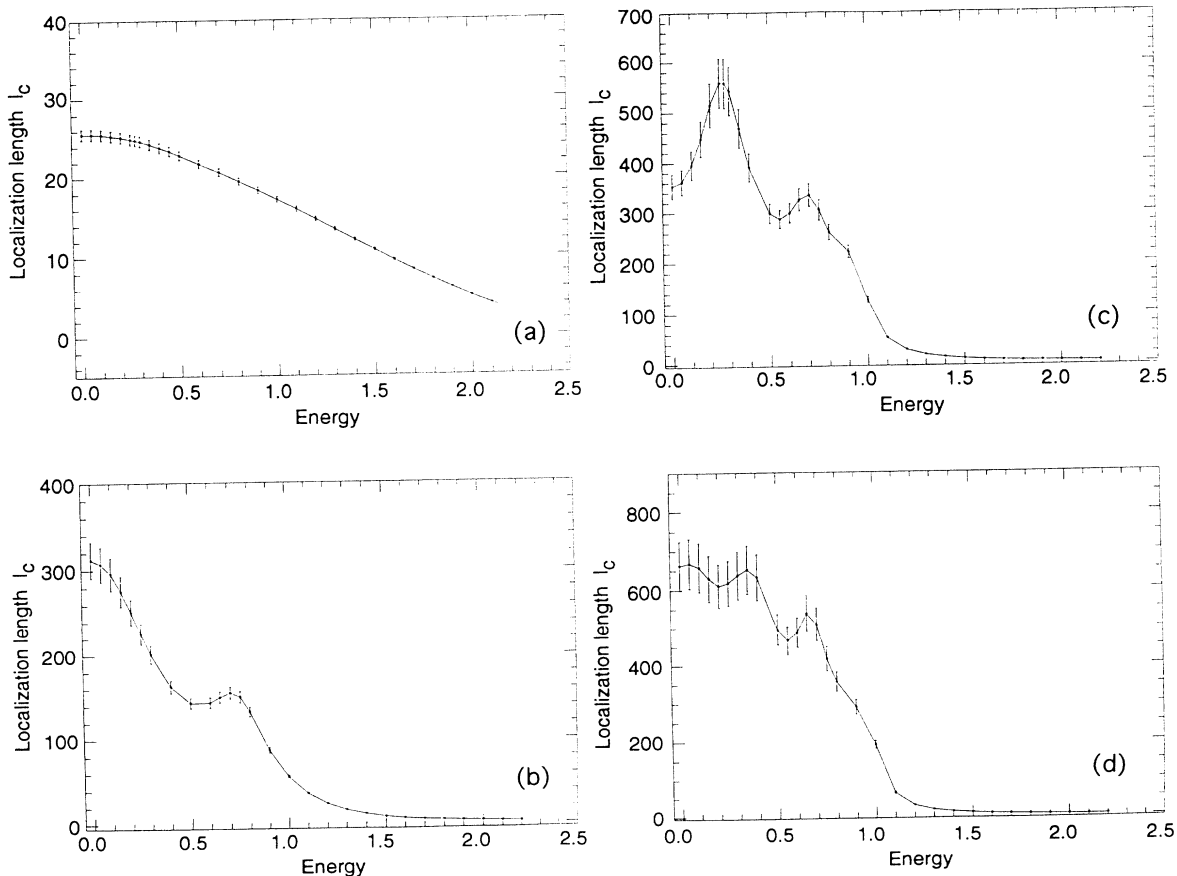


FIG. 3. The localization length  $\lambda$  versus energy for a random system of size  $N = 10\,000$ , disorder  $W = 2$ , and correlation length  $L = 1$  (a),  $L = 5$  (b),  $L = 10$  (c), and  $L = 15$  (d). The number of random configurations is  $M = 5000$ .

$L = 15$  in Fig. 2(d). As we will explain later, this structure is related to the finite correlation length  $L$ . It is well known that even for one rectangular barrier of width  $L$ , the transmission coefficient  $T$ , and the localization length  $\lambda$  which is related to  $T$  by  $T = \exp(-2L/\lambda)$ , shows strong dependence on energy, due to the presence of resonances. As we start increasing the disorder  $W$ , one notices that the structure in the energy dependence of the localization length  $\lambda$  is getting smaller. In Fig. 3 we present the results of  $\lambda$  for  $W = 2$  and in Fig. 4 we present the results of  $\lambda$  for  $W = 3$ , where only one maximum in  $\lambda$  has survived for values of  $L$ ,  $L = 5, 10$ . Finally, for a stronger disorder,  $W = 5$ . In Fig. 5 the behavior of  $\lambda$  versus  $E$  is the same for the uncorrelated case [Fig. 5(a)] as well as for the correlated case.  $\lambda$  has a maximum at  $E = 0$  and decreases monotonically as  $E$  approaches the end of the band ( $E = 2$ ).

In this section, we attempt to interpret the basic features shown in Figs. 2–5, i.e., the positions of the peaks of  $\lambda$  for different correlation lengths  $L$  and their gradual disappearance as the strength of the disorder  $W$  increases. We calculate the transmission coefficient for the 1D tight-binding model, with nonzero lattice energies,  $\epsilon_n = \epsilon_0$ , only in a section of the lattice of length equal to the correlation length  $L$ . This is analogous to the transmission studies through a potential barrier in the

continuous case.<sup>14</sup> In the continuous case, the transmission is well defined and not exponentially small when the energy is larger than the height of the potential barrier. In our discrete case of the tight-binding model, we have transmission when the incident energy lies both within the unperturbed band width, which ranges from  $-2$  to  $+2$ , as well as within the perturbed band width, which ranges from  $\epsilon_0 - 2$  to  $\epsilon_0 + 2$ . Therefore, for  $\epsilon_0 > 0$ , the allowed energies that show nonexponential transmission lie within the energy range  $[\epsilon_0 - 2, 2]$  and for  $\epsilon_0 < 0$  the energy range is  $[-2, \epsilon_0 + 2]$ . The transmission coefficient for a discrete lattice of finite length  $L$  with site energies,  $\epsilon_n = \epsilon_0$ , embedded in an underlined lattice with  $\epsilon_n = 0$ , can be easily calculated by iterating the equation

$$\epsilon_n c_n + c_{n+1} + c_{n-1} = E c_n. \quad (3)$$

The amplitudes  $c_{L+2}$  and  $c_{L+3}$  of the eigenfunctions with eigenenergy  $E$  can be taken to be  $c_{L+2} = 1$  and  $c_{L+3} = e^{ika}$ , where  $E = 2 \cos ka$  and  $a$  is the lattice constant. Then one can calculate, through the recursion relations of Eq. (3), the amplitudes  $c_0$  and  $c_1$  and thus obtain the transmission coefficient  $T$  by the relation

$$T = \frac{|e^{2ika} - 1|^2}{|c_1 - c_0 e^{-ika}|^2}. \quad (4)$$

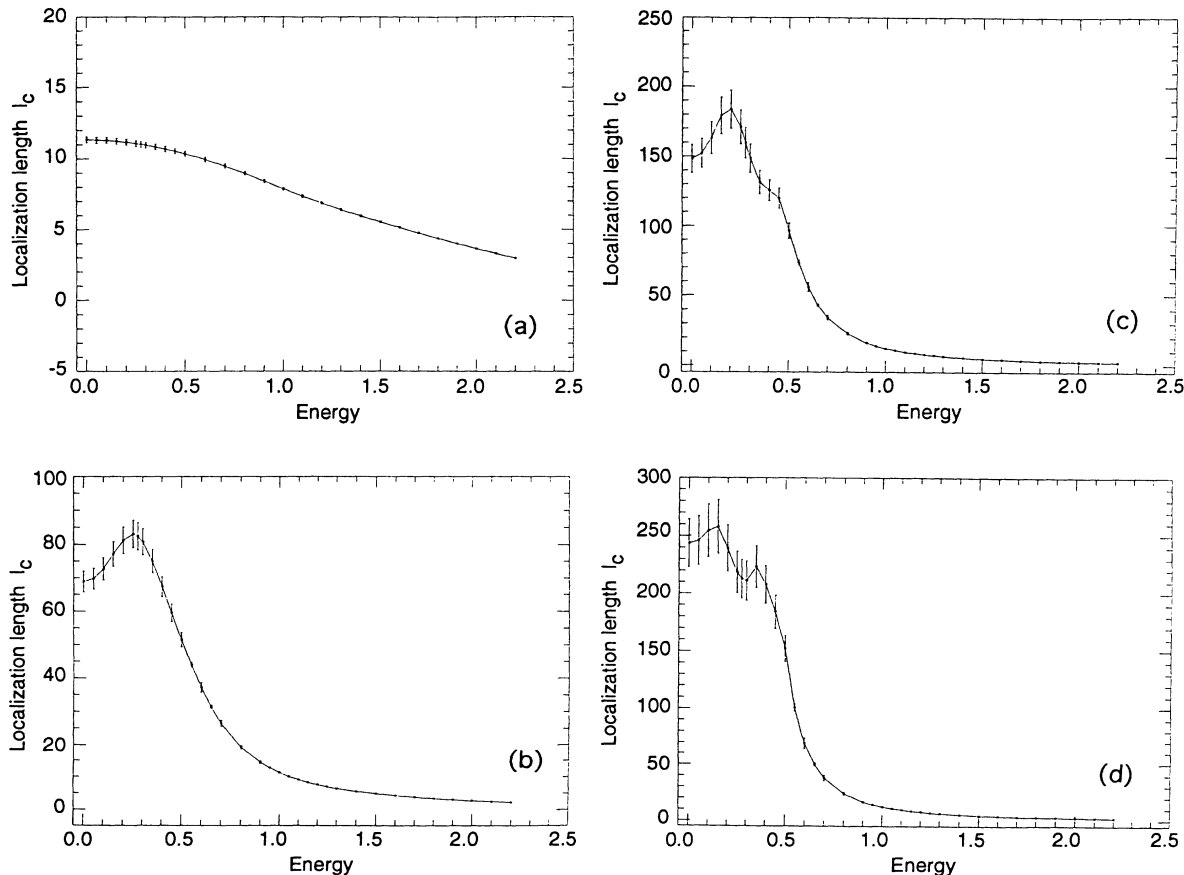


FIG. 4. The localization length  $\lambda$  versus energy for a random system of size  $N = 10\,000$ , disorder  $W = 3$ , and correlation length  $L = 1$  (a),  $L = 5$  (b),  $L = 10$  (c), and  $L = 15$  (d). The number of random configurations is  $M = 5000$ .

We have numerically calculated  $T$  for a finite lattice of length  $L$ . Results for  $L = 1, 2, 3$  agree with analytical results.<sup>1,5,6</sup> For all cases of finite  $L$ , the transmission coefficient as a function of energy rises from zero, fluctuates between maxima ( $T = 1$ ) and minima, and approaches  $T = 0$  at  $E \geq 2$ . The number of maxima depends on  $L$ , while the energy positions of the maxima depend on the strength of the site energy  $\epsilon_0$ . To explain the results presented in Figs. 2–5, we also calculated  $T$  for a finite lattice of length equal to the correlation length  $L$ , for  $M$  configurations of different “potential barriers” of height  $\epsilon_0$ , which is chosen from a random rectangular probability distribution of width  $W$ . To obtain good statistics for  $T$ , we have chosen  $M=5000$ . The results are presented in Fig. 6 for the case of  $L = 10$ , for different disorders  $W = 1, 2, 3$ , and 5. Note that indeed the average of the transmission coefficient through different heights of rectangular barriers of width  $L$  gives results which agree with that of  $T$  through a lattice of length  $N \gg L$  with correlated disorder. As the disorder  $W$  increases, the peaks in the transmission coefficient  $T$  become smaller and eventually they disappear when  $W = 5$ .

For the uncorrelated case, Thouless<sup>15</sup> has calculated the localization length  $\lambda$  within the second-order perturbation theory. The second-order perturbation result for

the localization length in the absence of correlation is  $\lambda_0 = [24(4 - E^2)]/W^2$ . We apply the same second-order perturbation treatment in our case, where the disorder is correlated. Following the discussion of Sec. IV of Ref. 4, we have that the average value of the square of the backward matrix element of the  $t$  matrix,  $\langle |T_b|^2 \rangle$ , is given by

$$\langle |T_b|^2 \rangle = \sum_{n,m} e^{2ik(n-m)} \langle \epsilon_n \epsilon_m \rangle. \quad (5)$$

For our correlated disorder, the double summation can be easily calculated and we obtain

$$\begin{aligned} \langle |T_b|^2 \rangle &= L \langle \epsilon^2 \rangle \left( 1 + \sum_{n=1}^{L-1} 2 \cos(kn) - \frac{2}{L} \sum_{n=1}^{L-1} n \cos(kn) \right) \\ &= L \langle \epsilon^2 \rangle \frac{\sin^2(kL)}{L \sin^2 k}. \end{aligned} \quad (6)$$

Then we can relate the reflection coefficient  $R$  to  $|T_b|^2$  (i.e.,  $R = |r|^2 = |G|^2 |T_b|^2$ , where  $G$  is the unperturbed Green’s function,  $G = -i/[(4 - E^2)^{1/2}]$ ). The localization length  $\lambda$  is then obtained from the relation  $1/\lambda = \langle |r|^2 \rangle / 2L$ . Finally, we obtain

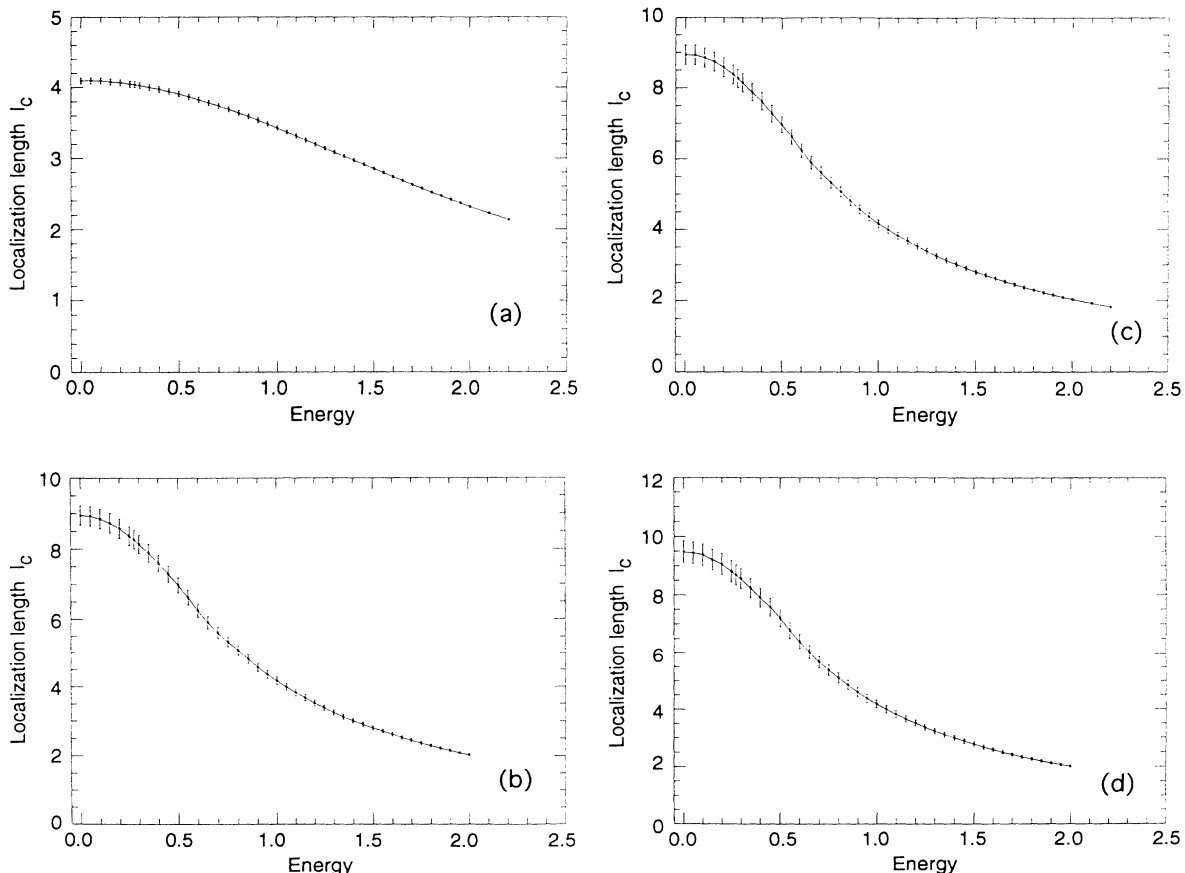


FIG. 5. The localization length  $\lambda$  versus energy for a random system of size  $N = 10\,000$ , disorder  $W = 5$ , and correlation length  $L = 1$  (a),  $L = 5$  (b),  $L = 10$  (c), and  $L = 15$  (d). The number of random configurations is  $M = 5000$ .

$$\frac{\lambda}{\lambda_0} = \frac{L \sin^2(k)}{\sin^2(kL)}, \quad (7)$$

where  $\lambda_0$  is the second-order perturbation result for the localization length in the absence of correlations. Therefore, we see that the introduction of correlations increases, in general,  $\lambda$  and also gives peaks in the energy dependence of  $\lambda$ . However, within the lowest order in perturbation,  $\lambda$  diverges at particular energies, while our numerical results give maxima in  $\lambda$ . In addition, the second-order perturbation result [Eq. (7)] is independent of  $W$ , all the disorder dependence of  $\lambda$  is through  $\lambda_0$ . So the perturbation theory result of Eq. (7) works only qualitatively in explaining our numerical results in Figs. 2–5. It gives maxima in the energy dependence of  $\lambda$ , but the positions do not exactly match those of Figs. 2–5.

In Fig. 7, we present results for the average DOS versus energy for the uncorrelated ( $L = 1$ ) and for the correlated disorder case ( $L = 10$  and  $L = 20$ ) for  $W = 1$ . Note that as the correlation length  $L$  increases, the sharp structure in the DOS in the band edges becomes smaller and the band size increases. This is the major effect of the corre-

lation on the DOS. As  $L$  increases, the structure in the DOS can be analyzed as follows. One obtains a superposition of different band widths, which span continuously from  $[-\frac{W}{2} - 2]$  to  $[\frac{W}{2} + 2]$ . This superposition of different bands is responsible for the widening of the total band, as well as the DOS around the  $E = \pm 2$ .

The energy level spacing distribution  $P(S)$  has been used<sup>9–13</sup> as a criterion in distinguishing localized states, which follow the Poisson distribution [ $P(S) = \frac{1}{D} \exp(-S/D)$ , where  $D$  is the mean energy spacing] from extended states, which follow the Wigner distribution [ $P(S) = \frac{\pi}{2} \frac{S}{D^2} \exp(-\pi S^2/4D^2)$ ]. In the uncorrelated case, numerical studies of  $P(S)$  show that indeed  $P(S)$  crosses over from Wigner-like distribution to a Poisson-like distribution, as the size of the system increases from below the localization length to well above it. This is clearly shown in Fig. 8 where  $P(S)$  is plotted for the uncorrelated case with  $W = 2$  and  $N = 20$  [Fig. 8(a)],  $N = 30$  [Fig. 8(b)], and  $N = 200$  [Fig. 8(c)]. When  $N = 20$  and/or  $N = 30$ , one clearly sees that  $P(S)$  follows the Wigner probability distribution, since for this case  $N \ll \lambda$ . We still have localization in our 1D system but  $\lambda$  is larger than the size of the system  $N$ . If

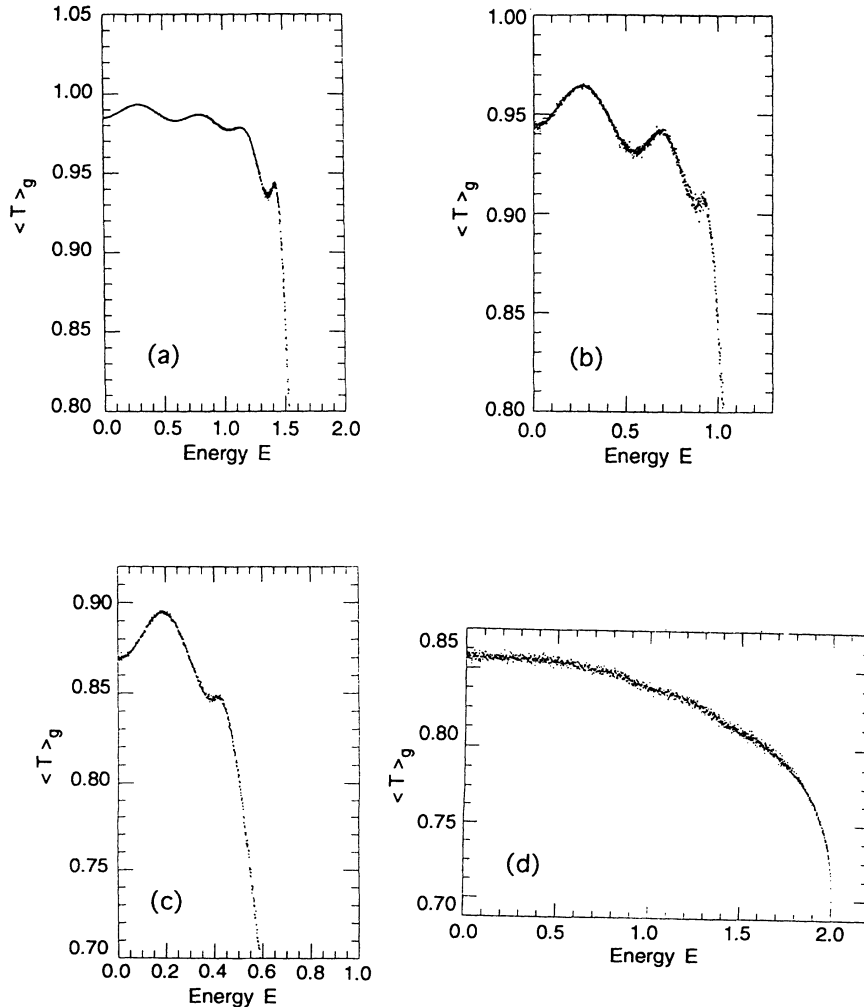


FIG. 6. The average transmission coefficient  $T$  versus energy for a random potential barrier of width  $L = 10$ , and random height of amplitude  $W = 1$  (a),  $W = 2$  (b),  $W = 3$  (c), and  $W = 5$  (d). The number of random configurations is  $M = 5000$ .

we keep the disorder  $W$  constant equal to 2 but increase the size of our system to  $N = 200$ , then one clearly sees the localization behavior through  $P(S)$ , which now follows the Poisson distribution [see Fig. 8(c)]. It will be interesting to examine  $P(S)$  in the presence of correlations. Following the previous argument one expects  $P(S)$  for the correlated disorder to follow mostly the Wigner

probability distribution. We have seen in Figs. 2–5 that the localization length  $\lambda$  increases dramatically for all the energies in the presence of correlations. We have mostly studied cases where  $N < \lambda$ , because of numerical difficulties, and this trend has been seen in Fig. 9(a), where we plotted  $P(S)$  for  $N = 100$ ,  $W = 2$ , and  $L = 5$ . In Fig. 9(b), we have plotted  $P(S)$  for  $N = 500$ ,  $W = 2$ , and  $L = 5$  and one clearly sees that  $P(S)$  comes closer to the Poisson rather than the Wigner probability distribution. Therefore, we see that the effects of the correlation are more pronounced on the localization length than in the DOS or  $P(S)$ .

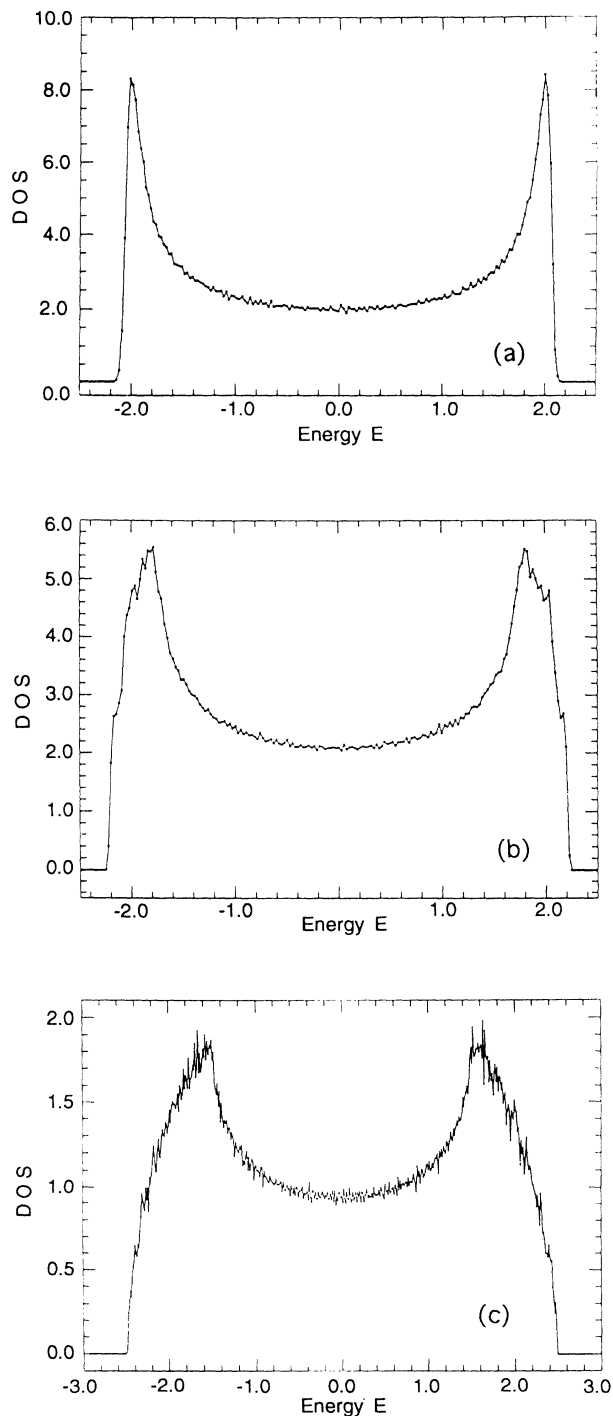


FIG. 7. Density of states averaged over  $M = 200$  configurations versus energy for a correlated random system.  $W = 1$  and  $L = 1$  (a),  $L = 10$  (b), and  $L = 20$  (c).

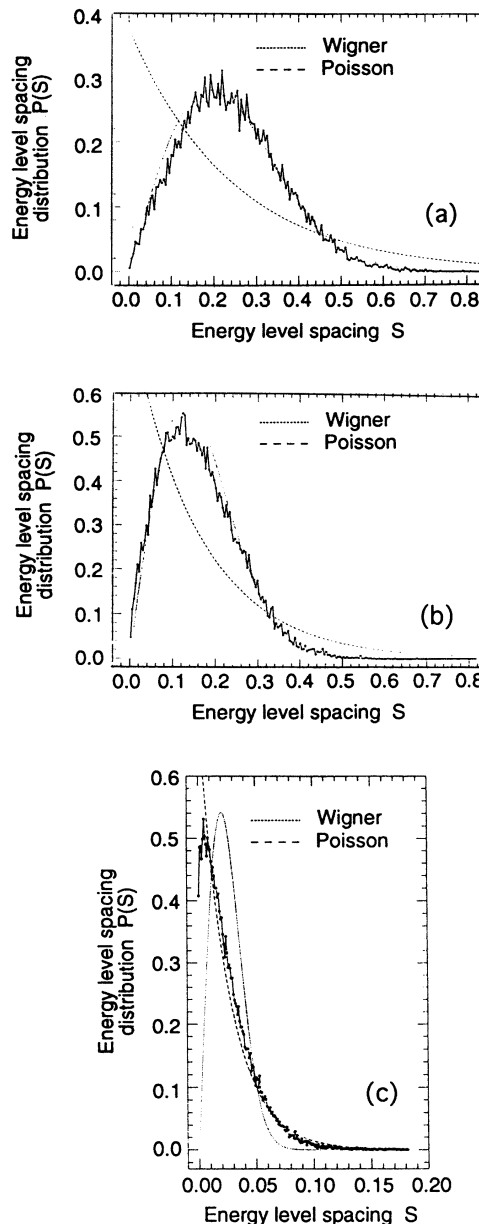


FIG. 8. Level spacing distribution  $P(S)$  for a fixed disorder  $W = 2$ , correlation length  $L = 1$  (uncorrelated case) and various system sizes  $N = 20$  (a),  $N = 30$  (b), and  $N = 200$  (c).

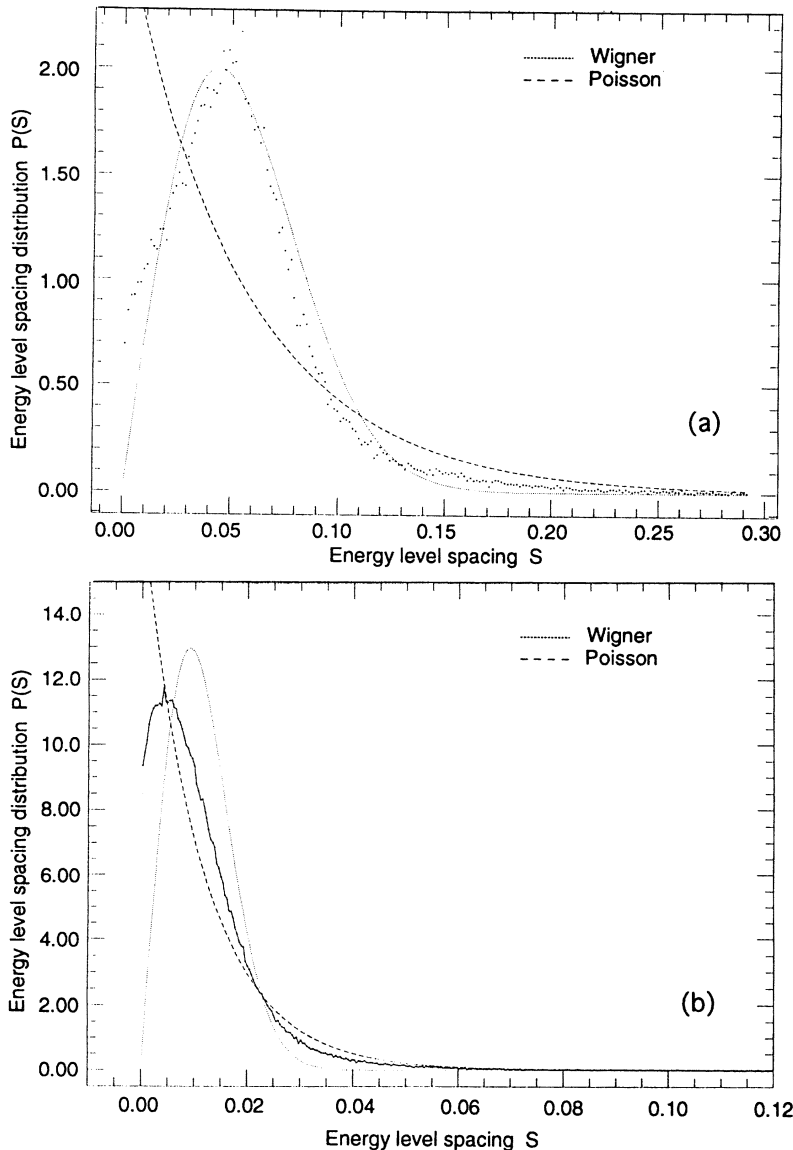


FIG. 9. Level spacing distribution  $P(S)$  for a fixed disorder  $W = 2$ , correlation length  $L = 5$ , and two system sizes  $N = 100$  (a) and  $N = 500$  (b).

#### IV. CONCLUSIONS

We have studied a tight-binding model with correlated random site energies of a smooth and simple probability distribution. Our purpose was to check the sensitivity of the results of the localization theory of 1D disordered systems to the effects of this correlation.

We found that the localization length increases as the correlation length  $L$  increases. A new structure in the energy dependence of  $\lambda$  was found, which is related to the transmission resonances of isolated potential barriers of width equal to  $L$ . Second-order perturbation theory for the correlated disorder accounts qualitatively for most of the structure in the localization length. By increasing the correlation, the structure of the DOS around the band edges smoothes out and the band widens. In the presence of correlation, the energy level spacing distribution

$P(S)$  follows the Wigner distribution for “extendedlike” wave functions where  $N \leq \lambda$  and the Poisson distribution for localizedlike states when  $N > \lambda$ . Our  $P(S)$  results suggest that the role of the correlation length  $L$  is simply to replace the lattice spacing of our uncorrelated results.

#### ACKNOWLEDGMENTS

M. J. V. would like to thank Ames Laboratory and the Research Center of Crete for their hospitality during his stay, where this work has been done. Ames Laboratory is operated for the U.S. Department of Energy by Iowa State University under Contract No. W-7405-Eng.82. This work was supported in part by the NSF Grant No. INT-9117356.



- <sup>1</sup> See, e.g., E. N. Economou, *Green's Functions in Quantum Physics*, 2nd ed. (Springer-Verlag, Heidelberg, 1983).
- <sup>2</sup> M. Kasner and W. Weller, *Phys. Status Solidi B* **134**, 731 (1986).
- <sup>3</sup> R. Johnston and B. Kramer, *Z. Phys. B* **63**, 273 (1986).
- <sup>4</sup> E. N. Economou, C. M. Soukoulis, and M. H. Cohen, *Phys. Rev. B* **37**, 4399 (1988).
- <sup>5</sup> D. H. Dunlap, H. L. Wu, and P. W. Phillips, *Phys. Rev. Lett.* **65**, 88 (1990); H. L. Wu, W. Goff, and P. W. Phillips, *Phys. Rev. B* **45**, 1623 (1992).
- <sup>6</sup> S. N. Evangelou and A. Z. Wang, *Phys. Rev. B* **47**, 13 126 (1993).
- <sup>7</sup> C. M. Soukoulis, E. N. Economou, G. S. Grest, and M. H. Cohen, *Phys. Rev. Lett.* **62**, 575 (1989).
- <sup>8</sup> S. John, in *Photonic Band Gaps and Localization*, edited by C. M. Soukoulis (Plenum, New York, 1993), p. 1, and references therein.
- <sup>9</sup> U. Sivan and Y. Imry, *Phys. Rev. B* **35**, 6074 (1987).
- <sup>10</sup> I. Kh. Zharekesh, *Fiz. Tverd. Tela (Leningrad)* **31**, 118 (1989) [*Sov. Phys. Solid State* **31**, 65 (1989)].
- <sup>11</sup> B. Wischmann and E. Müller-Hartmann, *Z. Phys. B* **79**, 91 (1990).
- <sup>12</sup> S. N. Evangelou and E. N. Economou, *Phys. Rev. Lett.* **68**, 361 (1992).
- <sup>13</sup> B. I. Shkrovskii, B. Shapiro, B. R. Sears, P. Lambrianides, and H. B. Shore, *Phys. Rev. B* **47**, 11 487 (1993).
- <sup>14</sup> E. Merzbacher, in *Quantum Mechanics* (Wiley, New York, 1991), p. 105.
- <sup>15</sup> D. J. Thouless, *J. Phys. C* **5**, 77 (1972).